

Lawrence Berkeley National Laboratory

LBL Publications

Title

Actinide Corroles: Synthesis and Characterization of Thorium(IV) and Uranium(IV) bis(-chloride) Dimers

Permalink

<https://escholarship.org/uc/item/2pw9f59c>

Authors

Ward, Ashleigh L.
Buckley, Heather L.
Gryko, Daniel T.
et al.

Publication Date

2014

Actinide Corroles: Synthesis and Characterization of Thorium(IV) and Uranium(IV) bis(μ -chloride) Dimers

Ashleigh L. Ward,^a Heather L. Buckley,^a Daniel T. Gryko,^{b,c} Wayne W. Lukens,^d and John Arnold^{*a}

Received (in XXX, XXX) Xth XXXXXXXXXX 20XX, Accepted Xth XXXXXXXXXX 20XX

DOI: 10.1039/b000000x

The first synthesis and structural characterization of actinide corroles is presented. Thorium(IV) and uranium(IV) macrocycles of Mes₂(*p*-OMePh)corrole were synthesised and characterized by single-crystal X-ray diffraction, UV-Visible spectroscopy, variable-temperature ¹H NMR, ESI mass spectrometry and cyclic voltammetry.

The organometallic and coordination chemistry of actinides has become the subject of increasing interest over the past decade.^{[1](refs)} Despite this recent surge, the study in particular of non-aqueous actinides remains underexplored when compared to that of the s, p and d block or even lanthanides. A better understanding of the differences in covalency between the 4f and 5f elements, as well as actinide-ligand complex formation has direct implications for improving nuclear waste remediation schemes.^(ref) Additionally, current literature suggests that the actinides can offer reactivity modes different from both transition metals and lanthanides, offering new routes to the development of novel catalytic methodologies,^(ref) which provides ample motivation for expansion of this limited knowledge base.

Macrocyclic complexes of actinides, in particular of the uranyl cation, are well established in the literature and include a variety of ligands.^(ref) These include crown ethers, calixarenes and more recently "pacman" polypyrroles.^(ref) Of particular relevance to this work are the actinide porphyrins of thorium and uranium, which despite being first reported in the mid to late eighties, only comprise a body of nine structurally characterized complexes.^(ref)

Closely related to porphyrins are the triply anionic corroles. These macrocycles possess a smaller ring size, and thus a metal coordination site further from the plane of the ring, allowing for unique or enhanced reactivity.^(ref) Until recently, although an abundance of mid-to-late transition metal and main group corroles were known,^(ref) corrole complexes of much of the periodic table remained elusive. With the synthesis of an alkali metal salt metathesis reagent, a wider range of the periodic table has been opened, with early metal as well as lanthanide corroles being recently reported.^(ref) Herein, we report the synthesis and characterization of the first actinide corroles with U(IV) and Th(IV).

Both complexes, (Mes₂(*p*-OMePh)corrole)₂Th₂(μ -Cl₂)(DME)₂ (**1**) and (Mes₂(*p*-OMePh)corrole)₂U₂(μ -Cl₂)(DME)₂ (**2**), were synthesized via combination of the corresponding lithium corrole, (Mes₂(*p*-OMePh)corrole)Li₃·6THF,^(ref) with ThCl₄(DME)₂^(ref) and UCl₄ respectively in dimethoxyethane (DME) (Scheme 1). In the thorium case, the reaction resulted in precipitation of a purple solid from solution, while a dark red solution was observed for the uranium complex after stirring at room temperature for 24 hours. Evaporation of the solvent in vacuo, followed by

recrystallization from a mixture of dichloromethane (DCM) and hexanes, afforded the desired product as dark red needles (93% yield) for **1**, and dark pink needles (83% yield) for **2**. Single crystals suitable for X-ray diffraction of **1** were obtained via slow evaporation of a solution of **1** in DCM at -40 °C, while layering diffusion of hexanes into DCM at -40 °C was used for **2**.

Surprisingly, both actinide corroles crystallize as a bis(μ -chloride) dimers (Th(IV) in Figure 1 and U(IV) in Figure S#), with each metal centre bound by a fully deprotonated corrole, a molecule of DME and two chlorides. This is different from the lanthanide corroles as well as the actinide porphyrins, which possess monomeric structures.^(ref) The coordination geometry about the metal centres is dodecahedral, and both the metal-chloride (Th-Cl1 2.932(2) Å and Th-Cl2 2.886(1) Å; U1-Cl1 2.873(2) Å and U1-Cl2 2.840(1) Å) and metal-solvent (Th-O1 2.665(5) Å and Th1-O2 2.586(5) Å; U1-O1 2.659(6) Å and U1-O2 2.555(5) Å) distances are characteristic of that of other Th(IV)^{ref} and U(IV)^{ref} complexes. The Th1-Th1' distance of 4.7279(4) and the U1-U1' distance of 4.6621(5) Å are similar to those reported for other chloride diamond core Th(IV) and U(IV) compounds.^(ref) The average Th-N distance (2.39(1) Å) is longer than is typical for Th-amido but comparable to that of the Th porphyrin (2.40 Å).^(ref) Likewise, the average U-N distance of 2.33(1) Å is slightly shorter than the analogous uranium (IV)

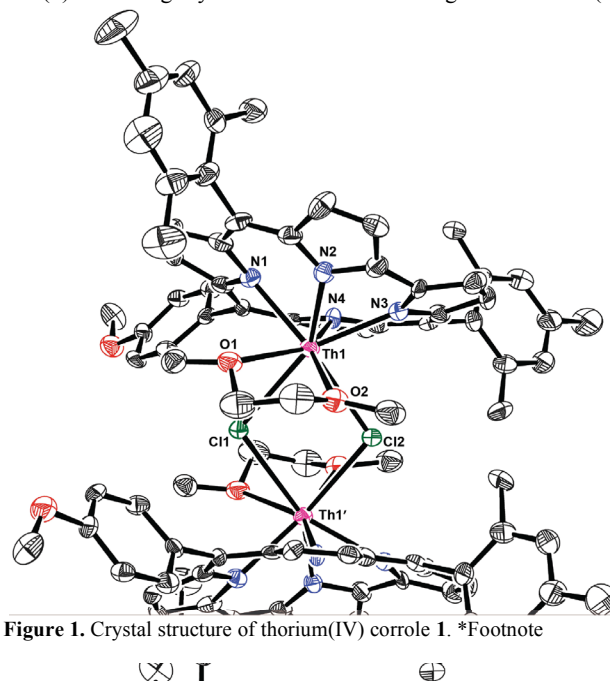
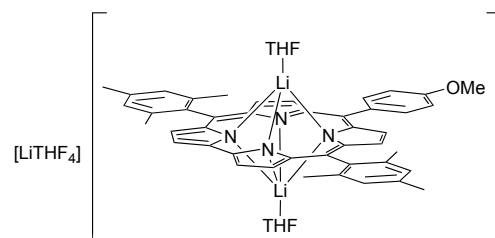
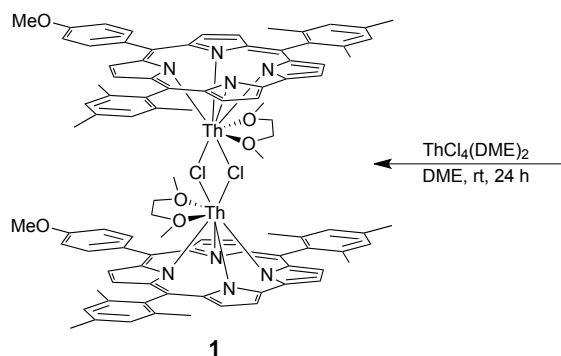


Figure 1. Crystal structure of thorium(IV) corrole **1**. *Footnote

porphyrin U-N distance at 2.41 Å. These distances are slightly



Scheme 1. Synthesis of thorium(IV) corrole **1** and uranium(IV) corrole **2**.



shorter than that of the Th-N corrole distance as is expected given the smaller ionic radius of U(IV).

The thorium centre is located 1.403 Å above the N₄ plane, as defined by the nitrogen atoms of the corrole, while the uranium is displaced by 1.330 Å. In **1**, metal-plane distance is slightly shorter than for that of the most closely related thorium porphyrin (1.403 Å vs. 1.424 Å), while the opposite is true for **2** (1.330 vs. 1.29 Å). This may seem surprising given the larger ring size of the porphyrin. However, other factors including the difference in ligand oxidation state (di- vs. tri-anionic), as well as the fact that in the solid state the porphyrin is a monomer and the corrole a dimer can be used to explain this trend. The U distance is slightly closer than the distance presented for the Th corrole, and is logical given their size differences. Apart from the aforementioned lanthanum corrole at 1.469 Å, these values are larger than any other metal N₄ plane distance for a corrole complex. The fact that the thorium and uranium are slightly closer to the corrole than the lanthanum is consistent with the difference in oxidation state, and thus ionic radius, between the two metals (La³⁺ vs. Th⁴⁺/U⁴⁺).

The actinide corroles display nearly identical UV-Visible spectra with each displaying one Soret band, 428 and 427 nm for **1** and **2** respectively. This single Soret peak is different from those observed for both the free-base and lithiated chromophores, and is indicative of a loss of planarity of the corrole. This is similar to that observed for Ga, Zr, and Al and the DME adducts of the analogous lanthanide corroles and is a result of the metal center sitting significantly above the plane of the ligand.(ref) Additionally, both **1** and **2** have two broad Q bands, 576 and 600 and 575 and 602 nm respectively. (can these be assigned?)

The electrochemical properties of actinide corroles **1** and **2**

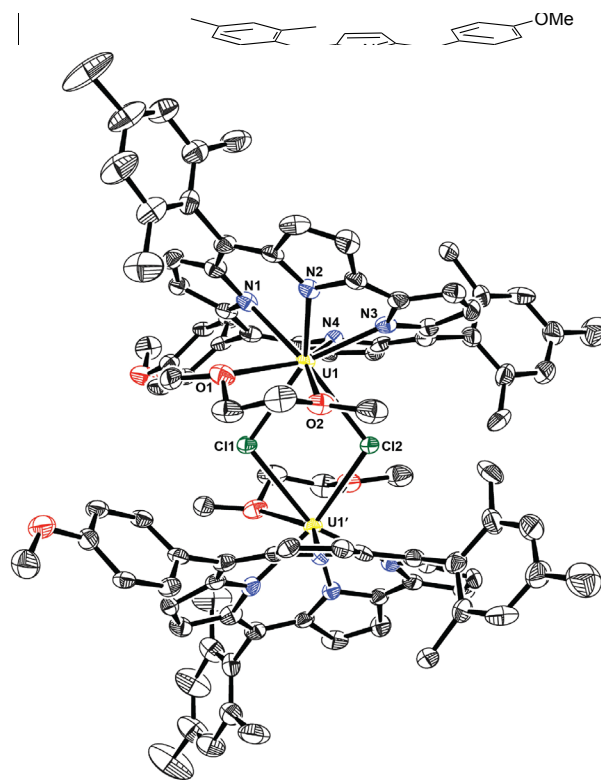


Figure 2. Crystal structure of uranium(IV) corrole **2**. *Footnote

were also examined. The cyclic voltammogram for the thorium corrole displays two reversible oxidations ($E_{1/2} = 124$ and 616 mV). Additionally there is an irreversible oxidative wave at 1.32 V. On the reductive side of the voltammogram there is an irreversible reduction at -1.81 V. Thorium(IV) is not known to display any redox behaviour within the potential range discussed here.(ref) Thus, the redox waves that are observed for complex **1** are ligand centred processes. However, the free base corrole does not display any redox behaviour inside the aforementioned window either. Therefore, the redox activity that is observed is attributed to ligand based behavior that arises due to the extreme distortion of the corrole ring from planarity that occurs when binding the actinides. Similar behaviour has been observed for the analogous bismuth corrole, which is also non-redox active.(ref)

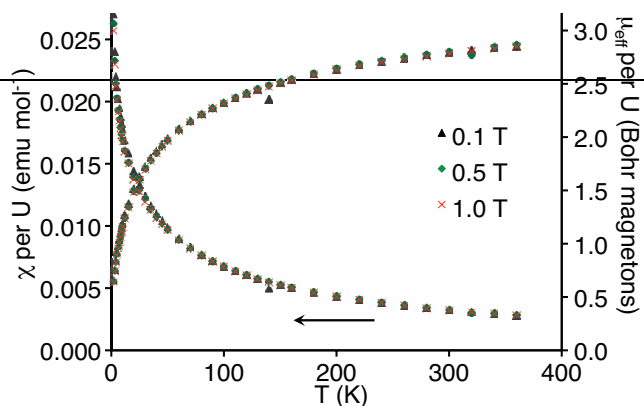
The cyclic voltammogram for **2** is more complicated. The first two oxidations seen for the uranium complex, which were reversible in the thorium case, are only quasireversible ($E_{1/2} = 124$ and 616 mV) and have additional oxidative shoulders ($E_{pa} = 0.44$ and 1.05 V). This behaviour is attributed to a monomer/dimer effect that is not as prominent in the case of **1**. Similar voltammograms have been observed for nickel porphyrins that also display a monomer dimer equilibrium.(ref) The oxidations are positively shifted for **2** when compared to **1**, which is expected given the greater distortion from planarity, and thus aromaticity, seen for the thorium complex, resulting in an increase in oxidation potential. Additionally, an irreversible oxidation at 1.54 V and a reduction at -1.85 V mirror those seen in the thorium case. The similarity in redox properties between the U(IV) and Th(IV) corroles has also been noted with actinide porphyrins and is attributed to the processes being ligand centred.

The ambient temperature ^1H NMR spectrum of **1** is straightforward in the aliphatic region. Four singlets can be assigned to the one p-methoxy, and three mesityl- CH_3 protons, as well as two additional singlets for the protons of the coordinated DME molecule. However, the resonances in the aromatic region are more complex than anticipated, displaying coalescence at room temperature. Upon cooling to -40 °C, the peaks in the aromatic region can be resolved. This dynamic solution behaviour is attributed both to the exchange of coordinating solvent and an equilibrium between the dimer that exists in the solid state and a monomer that is also present in solution. (Reference lanthanides?) As expected for a uranium(IV) compound, the proton resonances are broad and paramagnetically shifted for **2**. As with the thorium corrole, the signals that are broad due to fluxional behaviour sharpen upon cooling to -40 °C. Similar observations have been made for the analogous lanthanide corroles.(ref)

Variable temperature magnetic moment of **2** (Figure 3), is in good agreement with that expected for U(IV), which possess a $^3\text{H}_4$ ground state. At low temperature, the magnetic moment tends towards zero, which is consistent with an orbital singlet ground state ($m_j = 0$), which is typical of U(IV) complexes.(ref. Edelstein, N.M. and Lander, G.H. "Magnetic Properties" in "The Chemistry of the Actinide and Transactinide Elements, Third Edition" Morss, L.R.; Edelstein, N.M; and Fuger, J. eds. Springer: Dordrecht, 2006) Likewise, the magnetic moment at 360 K, $2.85 \mu_B$ is within the range observed for U(VI) amide complexes, $2.44 \mu_B$ to $3.48 \mu_B$. (refs: Stewart, J.L.; Andersen, R.A. *New J. Chem.* **1995**, *19*, 587-595 and Reynolds, J.G; Edelstein, N.M *Inorg. Chem.* **1977**, *16*, 2822-2825.) The reported magnetic moment for U(phthalocyanine) $_2$, ca. $3.1 \mu_B$, is also similar to that observed for **2**. (Lux, F.; Dempf, D.; Graw, D. *Angew. Chem. Int. ed Engl.* **1968**, *7*, 812-820)

Figure 3. Variable temperature magnetic susceptibility of uranium(IV) corrole **2**.

In brief, the synthesis and characterization of the first actinide corroles has been described. Given the broad range of non-aqueous actinide chemistry left to explore, the potential that these compounds have to provide a platform for the study of actinide bonding and reactivity is... Reactivity studies are on going to



determine the chemistry of these hitherto unavailable actinide macrocycles.

Notes and references

⁶⁰ ^a Department of Chemistry, University of California, Berkeley, California, 94720, United States. Tel: 001 510 643 5181; E-mail: arnold@berkeley.edu

^b Institute for Organic Chemistry, Polish Academy of Sciences, Warsaw, Poland. Tel: 48 22 3433063; E-mail: danielgryko@gmail.com

⁶⁵ ^c Warsaw University of Technology, Faculty of Chemistry, Warsaw, Poland.

^d Chemical Sciences Division, Lawrence Berkeley National Laboratory, Berkeley, California.

[†] Electronic Supplementary Information (ESI) available: Experimental procedures, electrochemical data, NMR data, crystal data, CIF files for **1** and **2**. See DOI: 10.1039/b000000x/

Acknowledgement: ALW acknowledges the NSF for a GFRP fellowship. DTG thanks the foundation for Polish Science. We are grateful to Antonio DiPasquale (XRD) and Zhongrui Zhou (MS) for assistance with instrumentation Andy Thomas. Portions of this work were supported by U.S. Department of Energy, Basic Energy Sciences, Chemical Sciences, Biosciences, and Geosciences Division and were performed at Lawrence Berkeley National Laboratory under Contract No. DE-AC02-05CH11231

[‡] Footnotes should appear here. These might include comments relevant to but not central to the matter under discussion, limited experimental and spectral data, and crystallographic data.

¹ A. Name, B. Name and C. Name, *Journal Title*, 2000, **35**, 3523; A. Name, B. Name and C. Name, *Journal Title*, 2000, **35**, 3523.

⁸⁵

DISCLAIMER

This document was prepared as an account of work sponsored by the United States Government. While this document is believed to contain correct information, neither the United States Government nor any agency thereof, nor the Regents of the University of California, nor any of their employees, makes any warranty, express or implied, or assumes any legal responsibility for the accuracy, completeness, or usefulness of any information, apparatus, product, or process disclosed, or represents that its use would not infringe privately owned rights. Reference herein to any specific commercial product, process, or service by its trade name, trademark, manufacturer, or otherwise, does not necessarily constitute or imply its endorsement, recommendation, or favoring by the United States Government or any agency thereof, or the Regents of the University of California. The views and opinions of authors expressed herein do not necessarily state or reflect those of the United States Government or any agency thereof or the Regents of the University of California.